Journal of Organometallic Chemistry, 300 (1986) 307–326
Elsevier Sequoia S.A., Lausanne – Printed in The Netherlands

ADVANCES IN THE CHEMISTRY OF HETERODIENE METAL COMPLEXES

K. VRIEZE

Anorganisch Chemisch Laboratorium, University of Amsterdam, J.H. van 't Hoff Instituut, Nieuwe Achtergracht 166, 1018 WV Amsterdam (The Netherlands)

(Received August 21st, 1985)

Summary

This review surveys recent advances in our research on the coordination chemistry of α-diimine metal compounds. Emphasis is placed on the novel developments in this field. Related work dealing with metal enimine compounds is also outlined.

It will be apparent from this review that we are interested not only in the coordination modes of α-diimines and enimines but also in the chemical activation of such ligands and in the influence of the coordinated ligands on the reactivity of the metal complexes.

Introduction

A rich chemistry has been developed in the field of the coordination of α-diimines. In our laboratory we have focused attention on the 1,4-diaza-1,3-butadienes RN=C(R')(R'')C=NR * (= R-DAB) and the 2-pyridinecarbaldehydeimines 2-$C_5H_4NC(R')$=NR (= R-Pyca). These ligands proved to be very interesting not only because of their versatile coordination behaviour, but also because of the wide variety of reactivity patterns. These properties are clearly related to the versatile nature of the ligands and to their electronic properties.

The versatile nature of the ligands originates in the fact that e.g. the R-DAB group may exist in the *E-s-trans-E* conformation, which is the ground state, in the *E-s-cis-E* conformation (Fig. 1), or in a *gauche* conformation with respect to the central C–C bond [1–3].

The structures of t-Bu-DAB [4] and of c-Hex-DAB have been determined by single crystal X-ray determinations [5]. The C=N and C=C bond lengths are 1.267(2) and 1.467(2) Å for t-Bu-DAB and 1.2576(22) and 1.4571(23) Å, respectively for the

* 1,4-Diaza-1,3-butadienes of the fomula RN=C(R')(R'')C=NR are abbreviated to R-DAB{R'; R''} [1–3], while the symbol R-DAB will be used for RN=C(H)(H)C=NR. The pyridylimine formulae 2-$C_5H_4NC(H)$=NR are abbreviated to R-Pyca.

0022-328X/86/$03.50

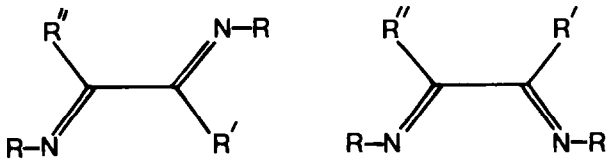

Fig. 1. The *E-s-trans-E* ground state conformation and the *E-s-cis-E* conformation of R-DAB.

c-Hex-DAB ligand. In both cases the molecule has a flat N=C–C=N skeleton in the *E-s-trans-E* conformation. Both the bond angles and the distances are typical for double N=C bonds and C(sp^2)–C(sp^2) bonds. Of interest is that unidentate σ-N coordination of the t-Bu-DAB in *trans*-$PdCl_2(PPh_3)$(t-Bu-DAB) does not influence to any appreciable extent the electronic structure of the ligand, since the C=N distances of the coordinated and non-coordinated moieties are 1.264(10) and 1.239(10) Å, respectively, with a central C–C distance of 1.485(9) Å [5]. Furthermore, the t-Bu-DAB still has a flat N=C–C=N skeleton with a *E-s-trans-E* conformation.

It was concluded from NMR spectra [6], dipole moments [7] and IR spectra [8] that in solution the R-DAB molecules predominantly exist in the *E-s-trans-E* conformation. In the gas phase the majority of the molecules of t-Bu-DAB have a *gauche* conformation with respect to the central C–C bond with a torsion of about 65° from the *s-cis* form [8,9].

With respect to the coordination properties of R-DAB and R-Pyca it is noteworthy that NDDO calculations of the LUMO energies indicate that the π-acceptor capacity increases in the order 2,2′-bipyridine < 2-pyridine-carbaldehyde-*N*-methylimine < R-DAB [10,11].

Finally, it is relevant to mention even at this stage that R-DAB and R-Pyca when coordinated to one or two metal atoms retain the flat conformation of the N=C–C=N skeleton remarkably well even when one or both C=N moieties are η^2-coordinated.

Possible coordination modes of R-DAB and R-Pyca ligands

In previous articles we have discussed extensively the various possible coordination modes of R-DAB ligands to one or more metal atoms. The most common types of coordination are shown in Scheme 1.

The R-DAB ligand in the unidentate coordination mode donates 2 electrons (σ-N; 2e). The ligand has the *E-s-trans-E* conformation, as it has in the (σ-N, σ-N′; 4e) donor mode. As a chelate R-DAB possesses the *E-s-cis-E* conformation, and it again uses 4e in the σ,σ-N,N′ coordination mode. The π and π* orbitals of the N=C–C=N system are sufficiently low in energy to be used for interaction with one or two metal atoms. As a result R-DAB may act as a (σ-N, μ_2-N′, η^2-C=N′) 6e donor and as a (σ-N, σ-N′, η^2-C=N, η^2-C=N′) 8e donor. In both cases the ligand has a virtually flat N=C–C=N skeleton in the *E-s-cis-E* conformation in order to allow chelation of the two N-atoms to one metal atom. For R-Pyca the 8e donor type of bonding has not been observed; this is not surprising, since such a bonding type would involve loss of resonance stabilization in the pyridine ring.

In the next section examples of the various types of coordination and furthermore the chemical activation of the coordinated R-DAB and R-Pyca ligands are discussed.

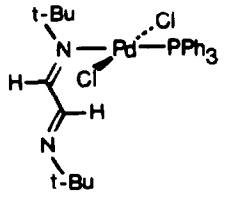

σ-N 2e

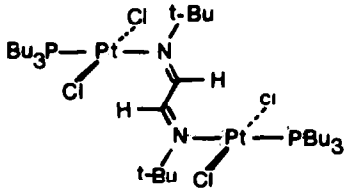

σ-N,σ-N' 2e,2e

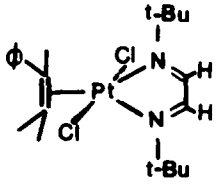

σ,σ-N,N' 4e

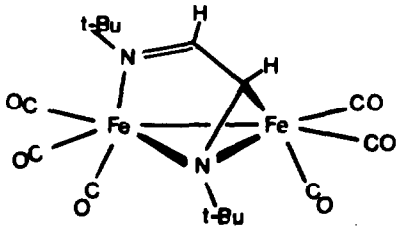

σ-N,μ^2-N',η^2-CN' 6e

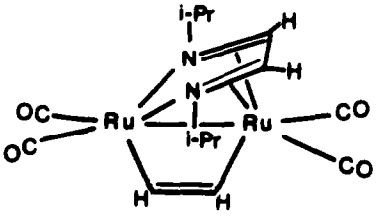

σ-N,σ-N',η^2-CN,η^2-CN' 8e

SCHEME 1. The most common coordination modes of R-DAB ligands

Reactions observed for the systems $Ru_3(CO)_{12}$/α-diimine (α-diimine is R-DAB or R-Pyca)

The reactions of $Ru_3(CO)_{12}$ with R-DAB provided an unique opportunity to investigate the role of the R group on the products formed and on the possible reaction routes [12–14]. The first isolable or observable intermediate in the reaction of $Ru_3(CO)_{12}$ with R-DAB is $Ru(CO)_3$(R-DAB). This species can be isolated, e.g.

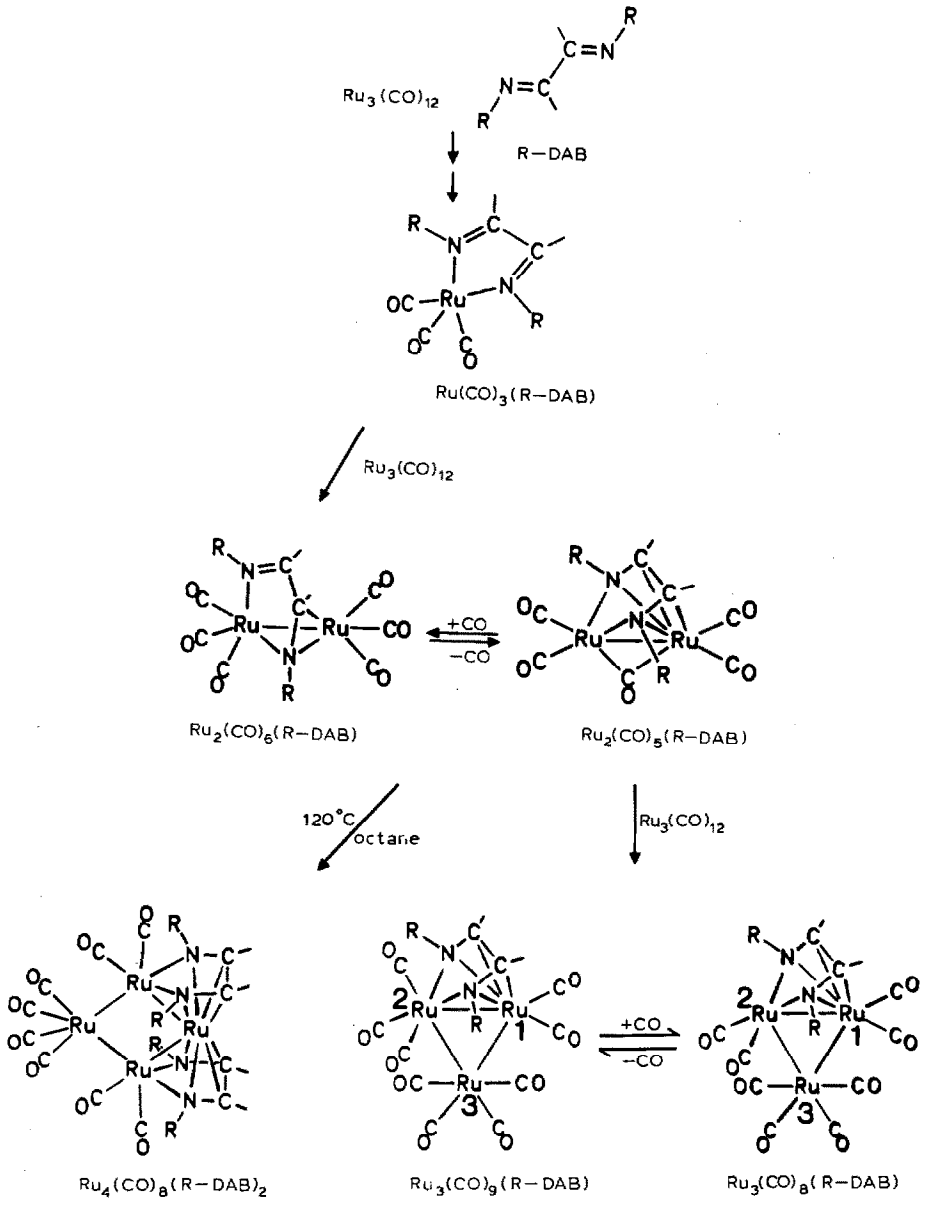

SCHEME 2. Reaction scheme for the system $Ru_3(CO)_{12}$/R-DAB.

when R is 2,6-Xyl, 2,4,6-Mes or $(i\text{-}Pr)_2Me$, i.e. for R groups which are branched in such a way that both C=N moieties are effectively screened against coordination by one or two metal atoms (Scheme 2).

For other R groups $Ru(CO)_3$(R-DAB) has been observed in solution. Such a compound is, however, very reactive, and when treated with $Ru_3(CO)_{12}$ forms $Ru_2(CO)_6$(R-DAB) (R = t-Bu, i-Pr, c-Hex) which contains a Ru–Ru bond, six terminal CO groups and a 6e donor R-DAB ligand. The structure is similar to that of $Fe_2(CO)_6$(c-Hex-DAB) [15]. When R is i-Pr or c-Hex, $Ru_2(CO)_5$(R-DAB) may

be formed by CO abstraction from $Ru_2(CO)_6$(R-DAB) or directly from $Ru_3(CO)_{12}$ and R-DAB for R is neo-Pe [13]. The crystal structure of $Ru_2(CO)_5$(i-Pr-DAB) showed the presence of a Ru–Ru bond (2.741(1) Å) bridged by one asymmetric bonded CO group and an 8e donor R-DAB ligand Scheme 2) [13]. The C=N and C–C bond lengths in the virtually flat N=C–C=N skeleton are 1.43(1) (mean) and 1.39(2) Å, respectively, indicating strong backbonding into the LUMO of the N=C–C=N system, which is bonding between the two C atoms and antibonding between the C and N atoms.

The complex $Ru_2(CO)_5$(R-DAB) reacts with many substrates. Thus reaction with CO rapidly gave $Ru_2(CO)_6$(R-DAB), as expected. Heating $Ru_2(CO)_5$(R-DAB) in octane gave very large yields of $Ru_4(CO)_8$(R-DAB)$_2$ (R = i-Pr, c-Hex, neo-Pe or i-Bu). The crystal structure of $Ru_4(CO)_8$(i-Pr-DAB)$_2$ shows a butterfly arrangement for the four Ru atoms [14]. There are four Ru–Ru bonds with bond lengths varying between 2.838(2) and 2.848(2) Å. Both R-DAB groups act as 8e donor ligands with C=N and C–C distances of 1.41(3) and 1.42(3) Å, respectively. These tetranuclear products may be thought of as having been formed by a very selective dimerisation reaction of two $Ru_2(CO)_4$(R-DAB) building blocks produced by dissociation of one CO from $Ru_2(CO)_5$(R-DAB). Treatment of $Ru_2(CO)_5$(R-DAB) with $Ru_3(CO)_{12}$ gave $Ru_3(CO)_9$(R-DAB) and $Ru_3(CO)_8$(R-DAB), where R = c-Hex, neo-Pe, or i-Bu (Scheme 2) [12]. The structure of the 48e cluster $Ru_3(CO)_8$(neo-Pe-DAB) shows, as expected, that the R-DAB ligand is in the 8e donor mode (C=N is 1.39(1) (mean) and C–C is 1.39 Å), while the Ru–Ru bond lengths are in the usual range (Ru(2)–Ru(1) 2.825(1); Ru(2)–Ru(3) 2.768(1) and Ru(1)–Ru(3) 2.737(1) Å) [16]. A notable aspect of the structure is that there is an obvious open coordination position on Ru(2), which may easily be filled by a CO group in a smooth reaction of $Ru_3(CO)_8$(R-DAB) with 1 atm of CO [12]. The crystal structure of the product $Ru_3(CO)_9$(R-DAB) (R = c-Hex) shows that the R-DAB is still in the 8e donor mode (C=N 1.39(1) (mean) and C–C 1.39(1) Å). No Ru–Ru bond in this 50e cluster is ruptured, but instead two Ru–Ru bonds are lengthened (Ru(2)–Ru(1) 3.026(1); Ru(2)–Ru(3) 2.956(1) and Ru(1)–Ru(3) 2.793(1) Å). It may be concluded that a low lying LUMO is present on the Ru_3 triangle in the green $Ru_3(CO)_8$(R-DAB), which may become occupied in the red $Ru_3(CO)_9$(R-DAB), causing bond lengthening in the metal–metal bonds connected to Ru(2) [12].

Reaction of $Ru_2(CO)_5$(R-DAB) with $Fe_2(CO)_9$ afforded $FeRu(CO)_6$(R-DAB) [13,17]. A crystal structure determination and the IR spectra of solutions of $FeRu(CO)_6$(i-Pr-DAB) showed that the structure is analogous to $M_2(CO)_6$(R-DAB) (M = Fe, Ru), while, interestingly, R-DAB appears to be σ-N=C coordinated to Ru and η^2-C=N (1.414(10) Å) coordinated to Fe. The Fe–Ru bond length is 2.6615(13) Å [13,17]. This indicates that Fe interacts more efficiently with the π-C=N bonds than Ru.

In the case of R-Pyca the 8e donor type of bonding appears to be very unlikely, as mentioned previously and so the reaction system $Ru_3(CO)_{12}$/R-Pyca is less complicated. It has been observed that $Ru_3(CO)_{12}$ with R-Pyca gives high yields of $Ru_2(CO)_6$(R-Pyca) with R = i-Pr, Hex or t-Bu [18]. The C=N moiety is in all cases η^2-bonded to one of the Ru atoms, while the pyridine N-atom is σ-N bonded to the other. The R-Pyca has a σ-N, μ^2-N′, η^2-C=N′ type of coordination mode. All reaction pathways leading to compounds with 8e donor α-diimine type of bonding are effectively blocked.

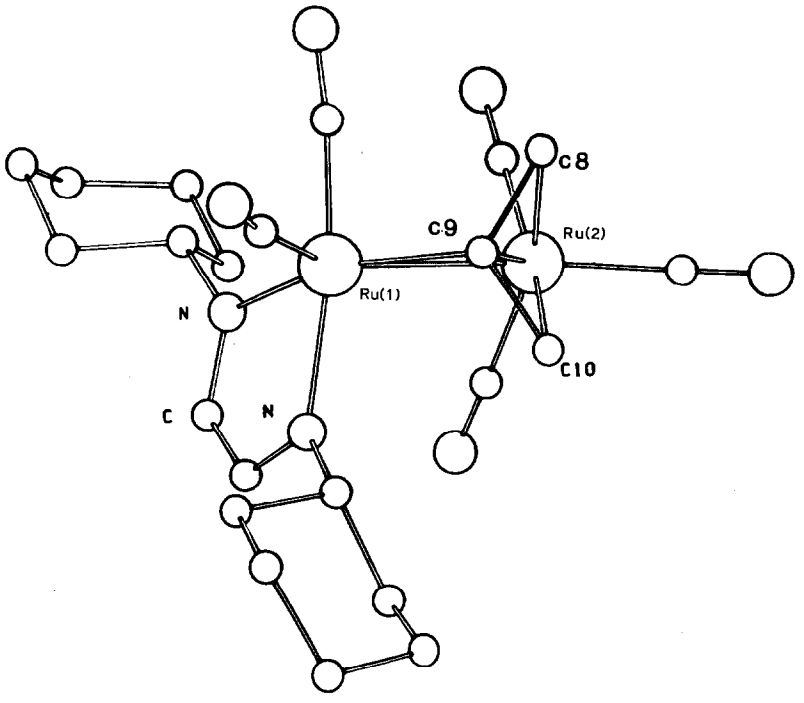

Fig. 2. Structure of $Ru_2(CO)_5$(c-Hex-DAB)(C_3H_4).

From the above it is clear that $Ru_2(CO)_5$(R-DAB) and $Ru_3(CO)_8$(R-DAB) are reactive compounds and prime candidates for further reactions. In the following sections the reactions of these compounds are discussed, and also the reactions of $Ru_2(CO)_6$(α-diimine) and $Fe_2(CO)_6$(α-diimine) (α-diimine = R-DAB or R-Pyca) with suitable substrates.

Reactions of $Ru_2(CO)_n$(R-DAB) ($n = 5$, 6), $Ru_2(CO)_6$(R-Pyca) and $Ru_3(CO)_8$(R-DAB) with allenes

Reaction of $Ru_2(CO)_6$(R-DAB) and of $Ru_2(CO)_6$(R-Pyca) (R = i-Pr, c-Hex) yielded compounds of the composition $Ru_2(CO)_5$(α-diimine)(C_3H_4). ^1H and ^{13}C NMR, IR, and crystal structure studies of $Ru_2(CO)_5$(c-Hex-DAB)(C_3H_4) and of $Ru_2(CO)_5$(c-Hex-Pyca)(C_3H_4) shows that the α-diimine is chelated to Ru(1) while the allene moiety is η^3-allyl bonded to Ru(2), with the central C atom of the allene linked to Ru(1). The Ru–Ru bond lengths are 2.812(3) and 2.8458(2) Å, respectively. The allene C–C distances are 1.44(3) (mean) and 1.41(1) Å (mean) for the c-Hex-DAB and c-Hex-Pyca derivatives, respectively [19]. The five CO groups are terminal, with two CO groups situated on Ru(1) and three on Ru(2) (Fig. 2).

The complex $Ru_3(CO)_8$(R-DAB) (R is neo-Pe) reacted with allene to form $Ru_3(CO)_7$(neo-Pe-DAB)(C_3H_4) [19]. A crystal structure determination showed this compound to contain a Ru_3 chain (Ru(1)–Ru(2) 2.736(9) and Ru(2)–Ru(3) 2.812(1) Å with a Ru(1)–Ru(2)–Ru(3) angle of 158° (Fig. 3)). The allene moiety is η^3-allyl bonded to Ru(3); (C(7)–C(8) 1.413(0) and C(8)–C(9) 1.490(0) Å), while the central

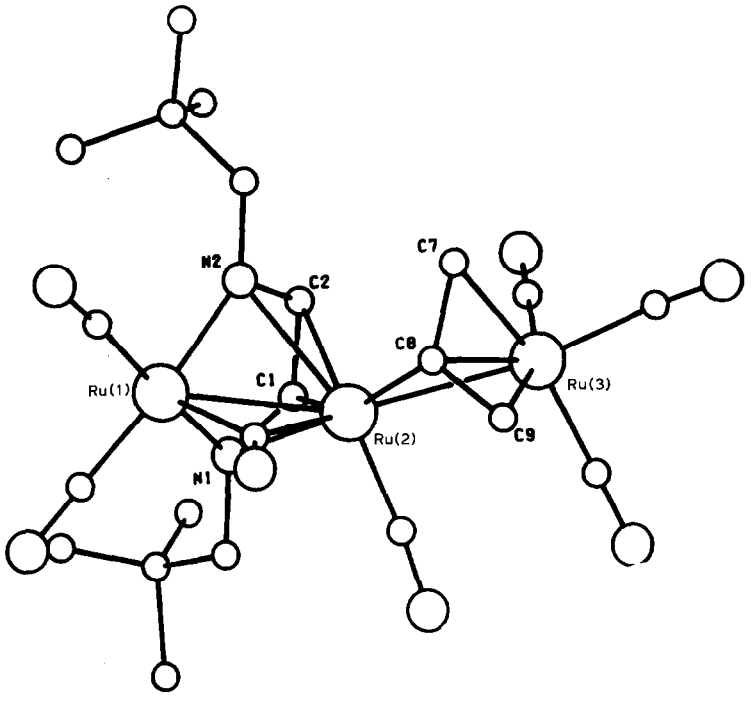

Fig. 3. Structure of $Ru_3(CO)_7$(neo-Pe-DAB)(C_3H_4).

C-atom of the allene unit is also bonded to Ru(2). The bonding of the neo-Pe-DAB unit is rather unusual, since there is no doubt that this R-DAB group is bonded as an 8e donor, but in an asymmetric fashion (C(1)–N(1) 1.345(0); C(2)–N(2) 1.336(8); C(1)–C(2) 1.415(5); Ru(1)–N(1) 2.123(3); Ru(1)–N(2) 2.162(5); Ru(2)–N(1) 2.329(1); Ru(2)–N(2) 2.500(1); Ru(2)–C(1) 2.198(4) and Ru(2)–C(2) 2.362(4) Å). The imine H-atoms resonate at unusually low fields, viz. at δ 6.97 and 6.14 ppm. In particular the first value is coming close to a 4e-donor chelated R-DAB group. The value of 6.14 ppm is as expected for an 8e-donor R-DAB group [3,16]. The ^{13}C resonances of the imine C-atoms appear at 117.8 and 100 ppm, respectively, which are fairly close to the expected values [3]. The reasons for the asymmetric bonding of the R-DAB group and of the η^3-allyl bonded allene group are not clear.

Reaction of $Ru_3(CO)_8$(R-DAB) with CH_2N_2

It was hoped that the empty coordination position on Ru(2) of $Ru_3(CO)_8$(R-DAB) (Scheme 2) could be utilized for the formation of a metal–carbene bond. However, reaction of $Ru_3(CO)_8$(R-DAB) with CH_2N_2 gave (μ-CH_2)$Ru_3(CO)_8$(R-DAB) [20]. The crystal structure for the case of R = neo-Pe showed that CH_2 had been inserted asymmetrically between Ru(2) and Ru(3) of $Ru_3(CO)_8$(R-DAB) (Scheme 2) (Ru(2)–C is 2.048(5); Ru(3)–C 2.204(6), while Ru(2) $\cdots$ Ru(3) is 2.1021(6) Å). The C=N and C–C distances are each 1.38(1) Å, indicating 8e donor bonding to the neo-Pe-DAB group in solution. The ^1H and ^{13}C NMR signals of the bridging CH_2 group appear at δ 3.7 and at 32 ppm, respectively, and are in line with observations for μ-C(H)R-bonded groups [21].

Reactions of $Ru_2(CO)_5$(R-DAB) and of $Ru_3(CO)_8$(R-DAB) with H_2

Both $Ru_2(CO)_5$(R-DAB) (R = i-Pr or c-Hex) and $Ru_2(CO)_6$(R-DAB) (R = i-Pr, c-Hex or t-Bu) gave $H_2Ru_2(CO)_5$(R-DAB) smoothly on treatment with molecular hydrogen at 1 atm [22]. The proposed structure for $H_2Ru_2(CO)_5$(R-DAB) is similar to that of $Ru_2(CO)_6$(R-DAB), the R-DAB acting as a 6e donor ligand. The two hydrogen atoms are located in *cis* disposition ($\delta(^1H)$ at -11.7 and -7.5 with J(H–H) of 6 Hz) on the Ru atom which is most accessible to outside attack, i.e. on the Ru-atom to which the imine moiety is σ-N=C coordinated.

The reaction of $Ru_3(CO)_8$(neo-Pe-DAB) with H_2 which leads to the formation of the known $H_4Ru_4(CO)_{12}$ and further of $H_2Ru_4(CO)_8$(R-DAB)$_2$ [22] is of special interest. The latter product contains a linear chain of four Ru atoms, corresponding to a total of 66 valence electrons (Fig. 4). The Ru(1)–Ru(2) distance is 2.806(2) the Ru(2)–Ru(2)* distance is 2.745(2) Å, with a Ru(1)–Ru(2)–Ru(2)* angle of 178.48(6)°. The Ru(1)–Ru(2) and Ru(1)*–Ru(2)* bonds are bridged by a flat 8e-donor R-DAB ligand with N=C and C–C bond lengths in the N=C–C=N skeleton of 1.35(2) and 1.39(2) Å respectively. The central Ru(2)–Ru(2)* bond is bridged by two carbonyl groups.

The intimate reaction mechanism leading to $H_2Ru_4(CO)_8$(R-DAB)$_2$ probably involves attack of H_2 on the open coordination position on Ru(2) of $Ru_3(CO)_8$(R-DAB) (Scheme 2). The following step would then require an oxidative-addition reaction with concomitant rupture of the Ru(2)–Ru(3) bond and formation of

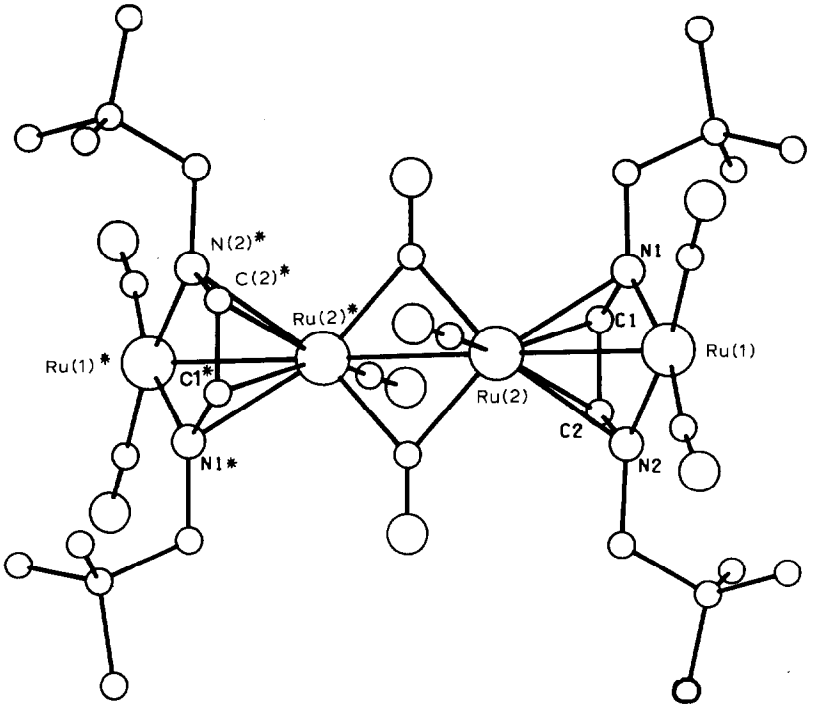

Fig. 4. Structure of $H_2Ru_4(CO)_8$(R-DAB)$_2$.

$HRu_2(CO)_4$(R-DAB), which dimerizes to $H_2Ru_4(CO)_8$(R-DAB)$_2$, and of $HRu(CO)_4$, which then tetramerizes to $H_4Ru_4(CO)_{12}$.

Reactions of coordinated α-diimines

The following sub-sections are concerned with the chemical reactivity of coordinated α-diimine ligands. It is now known that C–C, N–C, C–H and N–H bonds may be formed between R-DAB and other substrates.

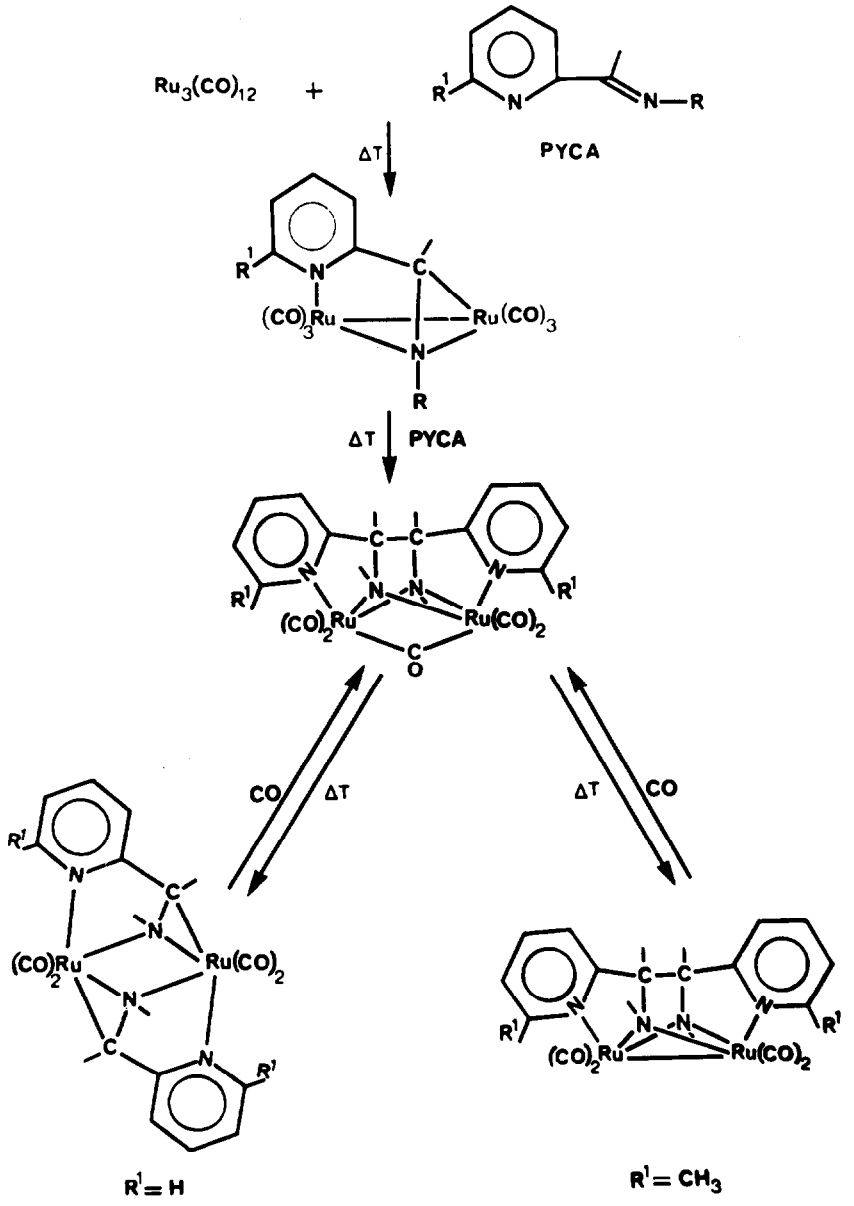

SCHEME 3. Reaction scheme for the system $Ru_3(CO)_{12}$/R-Pyca.

(i) Carbon–carbon coupling reactions

In previous reviews [1–3] the coupling of R-DAB groups, mediated by metal complexes to form the socalled IAE ligand, was discussed extensively (IAE denotes bis-[μ-1-(alkylamino)-2-(alkylamino)]ethane-*N*,*N*′) and so we consider here only the main points.

The first example of a compound containing such a tetradentate IAE ligand is $Mo_2(CO)_6$(IAE), which contains a Mo–Mo bonded pair (2.813(3) Å) with a bridging IAE ligand composed of two C–C coupled R-DAB groups (R = i-Pr, c-Hex or t-Bu) [23]. Each Mo atom has three terminal CO groups.

The formation of the IAE ligand and of the analogous APM ligand, which is formed by C–C coupling of two R-Pyca ligands (APM denotes bis-[μ-isopropylamino)-(2-pyridyl)-methane-*N*]) has also been observed for Ru. Reaction of $Ru_2(CO)_6$(α-diimine) (α-diimine = R-DAB with R = i-Pr, c-Hex or t-Bu, or R-Pyca with R = i-Pr, c-Hex or t-Bu) produced $Ru_2(CO)_5$(IAE) [24] and $Ru_2(CO)_5$(APM) [18], respectively. Scheme 3 shows, as an example, the reaction sequence for the coupling of two R-Pyca ligands.

Heating of $Ru_2(CO)_5$(IAE), which contains one bridging CO group and no metal–metal bond, gave $Ru_2(CO)_4$(IAE) with a Ru–Ru bond, and subsequently, by C–C bond rupture, the isomeric $Ru_2(CO)_4$(R-DAB)$_2$ with two 6e donor R-DAB groups. Heating of $Ru_2(CO)_5$(APM) in solution causes reaction via two pathways depending on the type of *ortho* substituent R′ on the pyridine ring (Scheme 3). When R′ is Me, only $Ru_2(CO)_4$(APM) was formed, and virtually no C–C bond rupture was observed. However, for R′ = H the $Ru_2(CO)_5$(APM) was directly transformed to $Ru_2(CO)_4$(R-Pyca)$_2$, probably via $Ru_2(CO)_4$(APM) as intermediate. It is noteworthy that $Ru_2(CO)_5$(APM) can be reformed by adding CO of 1 atm to $Ru_2(CO)_4$(R-Pyca)$_2$ (Scheme 3); such a reaction was not observed for $Ru_2(CO)_4$(R-DAB)$_2$ even when CO was used under pressure. It is of interest that this CO-promoted C–C coupling reaction occurs between two C atoms positioned on different metal atoms and on opposite sides of the Ru_2N_2 plane. The reaction probably involves initial formation of $Ru_2(CO)_5$(R-Pyca)$_2$ containing one bridging CO group, with the result that the C atoms which are to be coupled are brought into close proximity. In connection with the reaction schemes outlined above, it is relevant to mention that the crystal structures of $Ru_2(CO)_4$(i-Pr-DAB)$_2$ [24], $Ru_2(CO)_4$(i-Pr-Pyca)$_2$ [18] and of $Ru_2(CO)_5$(APM) (with R = i-Pr) [18] have been determined. The details are not further discussed here.

It was very recently shown that IAE formation also occurs with Mn complexes [25]. Reactions of $[(\eta^5\text{-}C_5H_5)Fe(CO)_2)]^-$ with $MnBr(CO)_3$(t-Bu-DAB) gave $Mn_2(CO)_6$(IAE) in addition to $Mn_2(CO)_6$(t-Bu-DAB). The complex $Mn_2(CO)_6$(t-Bu-DAB) deserves some comment, since it is the first compound in which the t-Bu-DAB ligand is bonded as an 8e donor. The structure was not determined, but

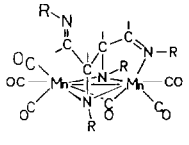

Fig. 5. Structure of $Mn_2(CO)_6$(IAE).

^{1}H NMR and IR data indicated that the complex is analogous to $Mn_2(CO)_6$(Me-DAB{Me,Me}) [26]. A crystal structure determination on $Mn_2(CO)_6$(IAE) showed that the IAE acts as an 8e donor ligand, since one of the imine N-atoms is not coordinated (Fig. 5) [25]. The Mn–Mn bond (2.58(6) Å) contains four terminal CO groups, one bridging CO group, and the terdentate IAE group. The two inequivalent imine N=C moieties are involved in a fluxional motion. SST NMR experiments indicated that the coordination modes of the two imine N-atoms exchange intramolecularly. The intermediate in this process involves probably a species with a 10e donor IAE ligand and without a Mn–Mn bond.

Finally, it should be mentioned that IAE and APM formation has also been observed in the case of organozinc compounds. Reaction of K[α-diimine] (α-diimine = R-DAB or R-Pyca) with EtZnCl gave high yields of Zn_2Et_2(IAE) and Zn_2Et_2(APM) [27]. The crystal structure of Zn_2Et_2(APM) with R = t-Bu showed a Zn_2Et_2 moiety bridged by a 10e donor IAE ligand. Both compounds are in an equilibrium with their monomeric paramagnetic persistent radical species [ZnEt(α-diimine)]$^{\cdot}$, as shown by variable temperature ESR spectroscopy [27,28]. The unpaired electron is mainly situated on the NCCN skeleton.

It is of interest that coupling of α-diimines to IAE (or APM) has now been realized for d^6, d^7, d^8 and d^{10} metals, indicating that it may possibly apply over more of the periodic system.

Carbon–carbon coupling reactions have also been observed between coordinated R-DAB ligands and other unsaturated systems. Reactions of $Ru_2(CO)_6$(R-DAB) (R = t-Bu) with R'N=C=NR' (R' = *p*-Tol, i-Pr, c-Hex) afforded by $Ru_2(CO)_5${t-BuN=C(H)(H)C(N-t-Bu)C(NR')=NR')} [29]. According to a crystal structure determination for R'-*p*-Tol, there is a Ru–Ru bond of 2.777(4) Å with one bridging CO group and four terminal CO groups. The carbodiimide ligand is coupled to the t-Bu-DAB ligand via a C–C bond of 1.53(1) Å. One N-atom of the carbodiimide is in a metal–metal bridging position, while the other N atom is not coordinated.

A rather similar product is formed from the reaction of $Ru_2(CO)_6$(R-DAB) (R = i-Pr, t-Bu or c-Hex) with thiofluorenone-*S*-oxide ($C_{12}H_8C$=S=O), which gave mainly $Ru_2(CO)_5${(R-DAB)-($C_{12}H_8CS$)} [29]. The crystal structure for R = i-Pr showed that the characteristic $Ru_2(CO)_5$ moiety is bridged by a $C_{12}H_8C$=S group, which is coupled to the i-Pr-DAB ligand via a C–C bond of 1.61(6) Å. The C=S bond is formally reduced to a single bond (1.91(4) Å). The Ru–Ru bond has a length of 2.810(7) Å.

It appears likely that the positively polarized C-atom (pseudo-allenic C centre) of R'N=C=NR' attacks the C-atom of the η^2-C=N bond of the R-DAB ligand which has gained more negative charge than the N-atom as a result of π-back-bonding. For the reaction with $C_{12}H_8CSO$ it may be assumed that the negatively charged O-atom reacts with the positively polarized C-atom of a CO group, resulting in formation of CO_2 and a thioketone moiety which then takes part in C–C coupling with the η^2-C=N bonded moiety of the R-DAB ligand [29].

Finally, we have also observed coupling of coordinated R-DAB ligands, with alkynes. The reactions of $Ru_2(CO)_n$(R-DAB) (n = 5, 6) with acetylene and mono- or di-substituted alkynes have been discussed extensively before [1–3,30]. Mono- and di-substituted alkynes form $Ru_2(CO)_5$(AIB), where AIB stands for 3-amino-4-imino-1-buten-1-yl. The crystal structure of $Ru_2(CO)_5$[t-Bu-DAB-PhC_2H)] shows that the alkyne is C–C coupled to the t-Bu-DAB ligand via the C–Ph end of the alkyne,

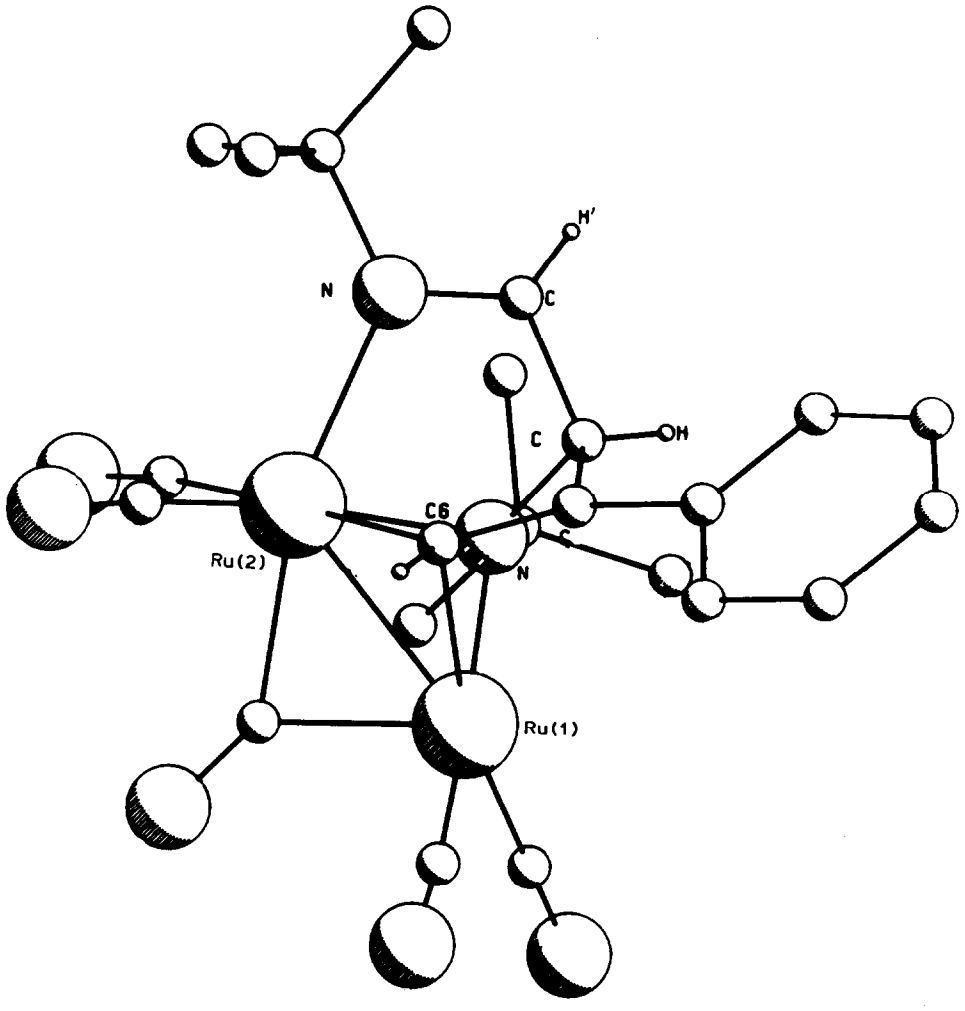

Fig. 6. Structure of $Ru_2(CO)_5$(t-Bu-DAB-PhC_2H).

while the C–H end of the alkyne bridges the Ru–Ru bond (2.711(1) Å). The new C–C bond thus formed is 1.546(10) Å. The alkyne triple bond is reduced to a double C=C bond (1.346(10) Å) (Fig. 6).

Further treatment of $Ru_2(CO)_5$(AIB) gave a catalytic selective cyclotrimerization to 1,3,5-trisubstituted benzenes when monosubstituted alkynes are utilized. The compounds $Ru_2(CO)_5$(AIB)(alkyne) and subsequently $Ru_2(CO)_4$(AIB)(alkyne) were characterized as intermediates [30].

Interestingly, use of $Ru_2(CO)_6$(R-Pyca) (R = t-Bu) with the alkyne HC_2-*p*-Tol did not give the type of compound discussed above, but instead $Ru_2(CO)_4$(t-Bu-Pyca)(HC=CRC(O)RC=CH) [18]. In Fig. 7 the molecular structure is given and shows that the R-Pyca has the chelating 4e donor mode while two alkynes together with one inserted CO form an organic moiety which donates 6e to the $Ru_2(CO)_4$(R-Pyca) moiety (Ru–Ru 2.737(3) Å). The triple bonds have been reduced

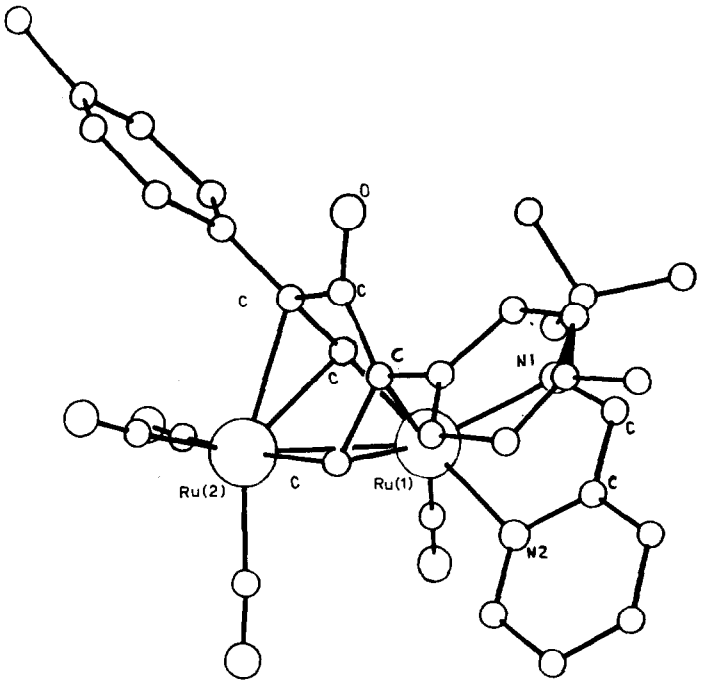

Fig. 7. Structure of $Ru_2(CO)_4\{(t\text{-Bu-Pyca})(HC{\equiv}CR)_2(CO)\}$.

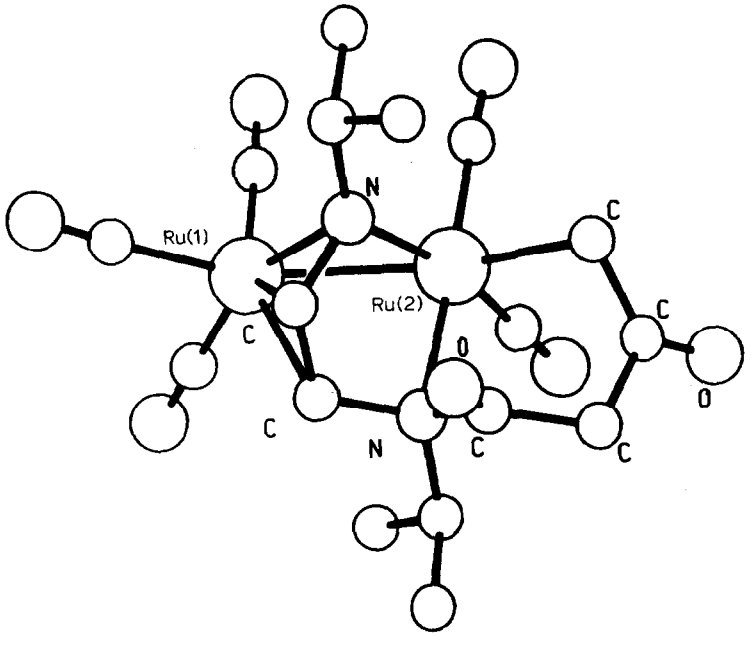

Fig. 8. Structure of $Ru_2(CO)_5[RNC(H)(H)CN(R)C(O)CH_2C(O)CH_2]$.

to double bonds, which both coordinate to a metal atom (C=C 1.44(1) Å (mean)). The ^{1}H NMR and IR spectra of the compound in solution are in accord with the solid structure. The structural features with respect to the bonding of the organic moiety are similar to those of $Fe_2(CO)_6(CH_3C_2CH_3)_2(CO)$ [31].

(ii) Nitrogen–carbon bond coupling reactions

Reaction of $Ru_2(CO)_6$(R-DAB) (R = i-Pr, c-Hex) with ketene $H_2C{=}C{=}O$ gives quantitative yields of $Ru_2(CO)_5[RNC(H)(H)CN(R)C(O)CH_2C(O)CH_2]$ [32]. According to a crystal structure determination for R = i-Pr, the molecule contains a $Ru_2(CO)_5$ moiety with only terminal CO groups, while the Ru–Ru bond (2.752(1) Å) is bridged by a 8e terdentate ligand formed via N–C coupling of the coordinated R-DAB ligand to a non-cyclic diketene group (Fig. 8). The RNCC unit in the DAB skeleton is η^3-azaallyl bonded to one Ru atom, while the other part of the ligand is a six-membered $RuCH_2C(O)CH_2C(O)N$(i-Pr) ring with a head-to-tail coupled diketene moiety. No reaction was observed between $Fe_2(CO)_6$(R-DAB) and ketene.

N–C coupling reactions have also been observed between $ZnEt_2$ and R-DAB [27]. These reactions have been discussed elsewhere [1–3,27] and will not be further considered here.

Cation–anion reactions involving metal R-DAB complexes

(i) Reactions without chemical activation of coordinated α-diimine

When the halide X^- in $MX(CO)_3$(R-DAB) (M = Mn, Re; X = Cl, Br, I; R = i-Pr, di-i-Pr$_2$-Me or *p*-Tol) is replaced by $[Mn(CO)_5]^-$ the compounds $(CO)_5MnM(CO)_3$(R-DAB) are formed in high yields [33]. The complexes contain a metal–metal bond and a chelating R-DAB ligand.

Replacement of Br in $MBr(CO)_3$(R-DAB) (M = Mn, Re; R = i-Pr, c-Hex or t-Bu) by $[Co(CO)_4]^-$ gave first the unstable $(CO)_4CoM(CO)_3$(R-DAB), and subsequently $MCo(CO)_6$(R-DAB) and CO [34]. The ^{1}H, ^{13}C NMR and IR data for the complexes and a crystal structure determination in the case of $MnCo(CO)_6$(t-Bu-DAB) make it clear that the compounds have a structure essentially similar to that of $Fe_2(CO)_6$(R-DAB) [15]. The $MM'(CO)_6$ moiety is bridged by a 6e donor R-DAB group with one N=C unit η^2-bonded to Co. The Mn–Co bond is 2.639(3) Å long, and is bridged by one semibridging CO group. It is evident that during the formation of the compound one CO group on Co in the intermediate $(CO)_4CoM(CO)_3$(R-DAB) is displaced by an imine moiety, which becomes η^2-bonded to Co.

A complicated set of reactions was observed when $MBr(CO)_3$(R-DAB), reacts with $[HFe(CO)_4]^-$, which is isoelectronic with $[Co(CO)_4]^-$.

A rather straightforward reaction involves the replacement of Br^- in $MBr(CO)_3$(R-Pyca) (M = Mn, R = i-Pr or t-Bu; M = Re, R = i-Pr) by $[HFe(CO)_4]^-$. The product is (μ-H)$FeM(CO)_6$(R-Pyca) which bears one bridging H atom and a 6e donor R-Pyca group, as confirmed by NMR spectroscopy and a crystal structure determination of (μ-H)$FeMn(CO)_6$(t-Bu-Pyca) [35] (Fig. 9B). The FeMn bond of 2.7465(3) Å is involved in an asymmetrically bent Fe–H–Mn interaction (Fe–H 1.61(2) and Mn–H 1.73(2) Å). The pyridyl N atom is σ-N bonded to Mn, while the imine N=C bond is η^2-bonded to Fe (N=C 1.408(2) Å). The H-atom gives a NMR signal at δ −16 ppm. The reaction route leading to this product is probably similar to that proposed for the formation of $MCo(CO)_6$(R-DAB). In the case of the Fe

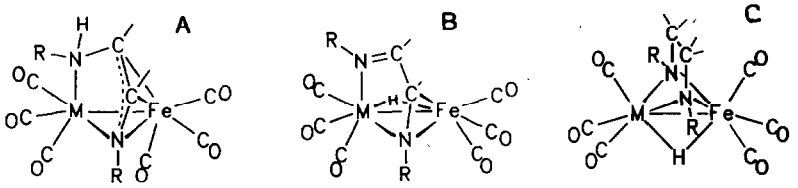

Fig. 9. Schematic structures of $FeM(CO)_6$(t-Bu-AAA) (**A**), (μ-H)$FeM(CO)_6$(α-diimine) (**B**) and (μ-H)$FeMn(CO)_6$(μ,μ'-*p*-TolNCH$_2$CH$_2$N-*p*-Tol) (**C**).

compound CO elimination with concomitant η^2-C=N coordination must be accompanied by a small movement of the H-atom to an asymmetric bridging position. In reactions of $ReBr(CO)_3$(R-DAB) (R = i-Pr or c-Hex; i-Pr-DAB{H;CH_3;}) with $[HFe(CO)_4]^-$ compounds (μ-H)$FeRe(CO)_6$(R-DAB) were formed [35], but the reaction route may be more complex than that observed for the R-Pyca metal complexes.

(ii) Reactions with chemical activation of coordinated R-DAB

In contrast to the reaction previously described it was found that $MBr(CO)_3$(t-Bu-DAB) (M = Mn, Re) reacted with $[HFe(CO)_4]^-$ to yield $FeM(CO)_6$(t-Bu-AAA), where t-Bu-AAA denotes 3-t-butylamino-1-t-butyl-1-azaallyl [36]. A crystal structure determination revealed that a $(CO)_3FeMn(CO)_3$ moiety is present with a short Fe–Mn bond of 2.628(4) Å (mean) (Fig. 9A), while five CO groups are terminal (three to Mn and two to Fe), and one CO group is semibridging. The NCC azaallylic moiety is η^3-bonded to Fe, with N–C and C–C bond lengths of 1.38 Å [36]. It was deduced from infrared data that a hydrogen atom is bonded to one N-atom of the R-DAB group (ν(N–H) 3290 cm^{-1}), while ν(N–D) was 2430 cm^{-1} when $[DFe(CO)_4]^-$ was used in the reaction.

In the case of $FeRe(CO)_6$(i-Pr-AAA) heating led to the formation of the isomeric hydride (μ-H)$Fe(CO)_6$(i-Pr-DAB) with a configuration analogous to that of (μ-H)$FeM(CO)_6$(R-Pyca) (Fig. 9B) [35]. This conversion is strictly a first order reaction with a standard energy of activation $\Delta G^{\ddagger}$ 27 kcal mol^{-1}. The conclusion is that in this case the hydride compound is thermodynamically more stable than the azaallylic complex.

It may further be concluded that the formation of the hydride complexes may proceed via two routes: (i) the azaallylic compound and (ii) a simple substitution reaction, as described in the previous subsection for the R-Pyca complexes, since azaallylic intermediates appear to be very unlikely for R-Pyca derivatives.

The intimate reaction mechanism for the formation of the azaallylic compounds $FeM(CO)_6${R-AAA} is not clear. In the first step Br in $MBr(CO)_3$(R-DAB) is replaced by $[HFe(CO)_4]^-$. The second step might be a double bond insertion of one C=N moiety into the Fe–H bond, followed by CO dissociation and formation of the η^3-azaallylic complex. An alternative route might involve a S.E.T. reaction in the intermediate $(CO)_3$(R-DAB)M-Fe(H)$(CO)_4$ taking place within the molecule with unpaired electrons localized on the R-DAB unit and on the H atom, respectively. The H may then migrate to one N-atom of the R-DAB group, since the spin density on the N atoms is probably higher than that on the imine C-atoms. Finally CO dissociation occurs, with formation of $FeM(CO)_3${R-AAA}. The reader is referred to the original publications for the proposed schemes [3,36].

Surprisingly, reaction of $MnBr(CO)_3$(*p*-Tol-DAB) with an excess of $[HFe(CO)_4]^-$ and subsequent protonation afforded (μ-H)$FeMn(CO)_6$(μ,μ'-Tol-NCH_2CH_2N-*p*-Tol). During the reaction the chelating R-DAB is reduced to the formally dianionic 8e donor 1,2-di-*p*(tolylamine)ethane group [37]. A crystal structure determination showed that a $FeMn(CO)_6$ moiety is present, with all CO groups in a terminal position, while the FeMn bond (2.5393(9) Å) is bridged by a H atom (Mn–H 1.70(6) and Fe–H 1.83(6) Å). The ^1H NMR signal of the bridging hydride appears at δ −10.02 ppm. The eighteen atoms of the *p*-Tol-NCH_2CH_2N-*p*-Tol skeleton are in one plane, perpendicular to the Fe–Mn bond (Fig. 9C). Use of $[DFe(CO)_4]^-$ with subsequent protonation gave (μ-H)$FeMn(CO)_6$\{μ,μ'-*p*-TolNC(H)DC(H)DCN-*p*-Tol\}. For the proposed reaction mechanism the reader is referred to the original publication [37], and it suffices to mention that the presence of the *p*-tolyl group on the N atoms of R-DAB may now induce a higher electron density on the imine C atoms than on the N atoms because of delocalization over the aryl rings. If an S.E.T. reaction occurred the H′ atom would then migrate to the C atoms [37]. The metal–metal bridging hydride arises from protonation by dilute acid or silica.

In addition to C–H and N–H bond formation, which have been discussed in this subsection it should be realized that $Mo_2(CO)_6$(IAE) [23] and $Mn_2(CO)_6$(IAE) [25] have been produced in reactions of $MnBr(CO)_3$(R-DAB) with $[Mo(CO)_4$(R-DAB)$]^-$ and with $[(\eta^5\text{-}C_5H_5)Fe(CO)_2]^-$, respectively. In these reactions, the products of which have been discussed previously, homo-dimetallic compounds are formed as the final products rather than hetero-dimetallic species. It is not at all clear which reaction mechanisms operate, but processes involving radical type intermediates might be feasible.

Reactions of $Ru_3(CO)_{12}$ with enimines $RN{=}C(H)(H)C{=}C(H)CH_3$

This review of our work would not be complete without mentioning some recent results on the reactions of $Ru_3(CO)_{12}$ with enimines [38]. This study is still in the exploratory phase, but is of interest in relation to the α-diimine work.

Reactions of $Ru_3(CO)_{12}$ with the enimines $RN{=}C(H)(H)C{=}C(H)CH_3$ (R = i-Pr, c-Hex or t-Bu) produce a number of products, the product ratio depending on R and on the reaction time, as shown by HPLC measurements.

In the case of R = t-Bu three products have been characterized i.e.: $Ru_2(CO)_5(RN{=}C(H){-}C{-}CH_2CH_3)$ (**A**), $Ru_2(CO)_6(RN{=}C(H)(H)C{=}C{=}CH_2)$ (**B**) and $Ru_4(CO)_{10}(RN{=}C(H)(H)C{=}C{-}CH_3)$ (**C**). In the case of R = i-Pr an unidentified compound and $Ru_2(CO)_6(RN{=}C(H)(H)_2CCCH_2)$ (**D**) are formed first. With longer reaction times it appears that the concentrations of these compounds decrease relative to those of the compounds $Ru_2(CO)_6(RN{=}C(H)(H)C{=}C{=}CH_2)$ (**B**) and $Ru_4(CO)_{10}(RN{=}C(H)(H)C{=}C{-}CH_3)$ (**C**), which are formed at a later stage. Compound **A** was not formed for R = i-Pr or c-Hex. For R = c-Hex the situation is as yet less clear, but four products are formed, analogous to those formed in the case of R = i-Pr. For all the R groups used the tetranuclear compound **C** is apparently the final and main product.

Crystal structures were determined for compounds **A** (R = t-Bu), **B** (R = t-Bu) and **C** (R = i-Pr), while the molecular configuration of **D** (R = i-Pr or c-Hex) was deduced from extensive NMR and IR investigations (see Figs. 10–13).

Compound **A** (t-Bu) (Fig. 10) consists of a $Ru_2(CO)_6$ fragment with terminal CO

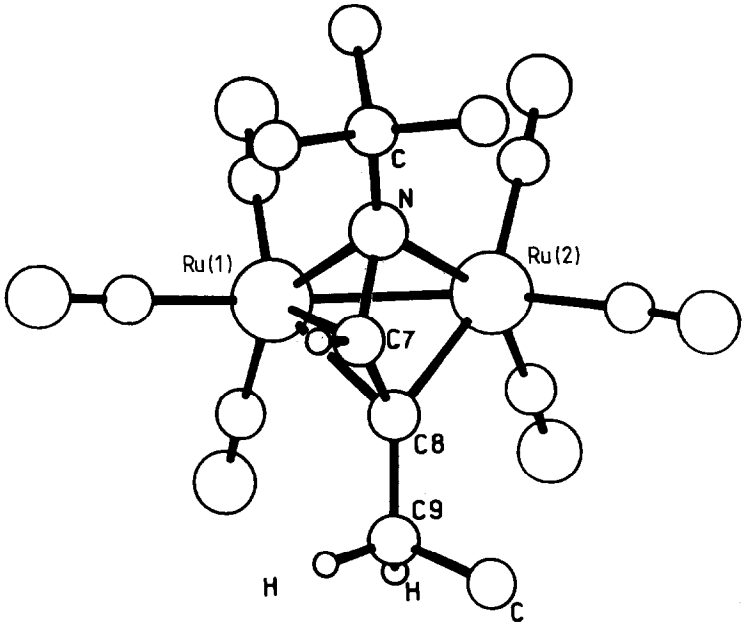

Fig. 10. Structure of $Ru_2(CO)_6$(t-Bu-N=C(H)=CCH_2CH_3).

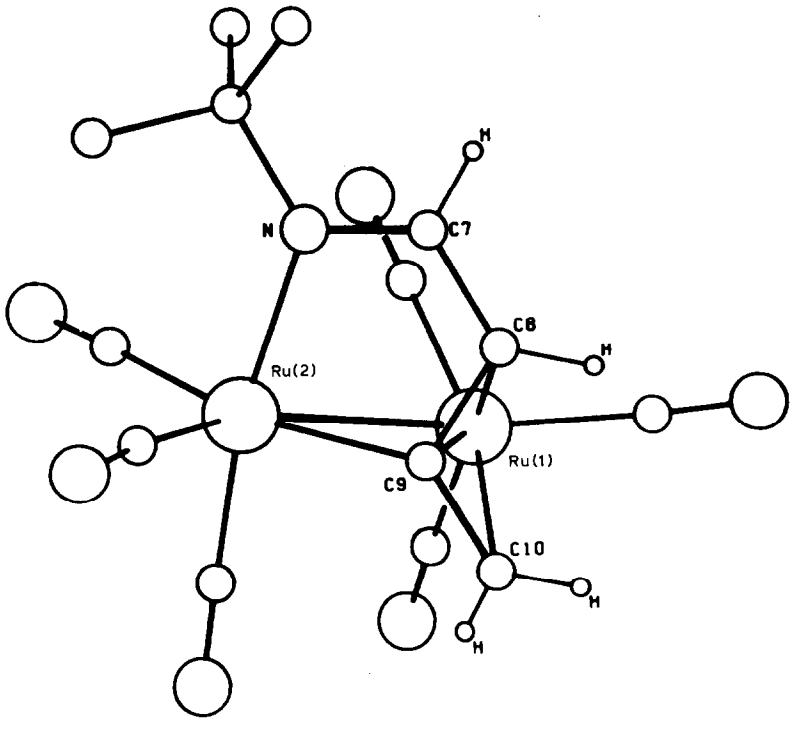

Fig. 11. Structure of $Ru_2(CO)_6$(t-Bu-N=C(H)(H)C=C=CH_2).

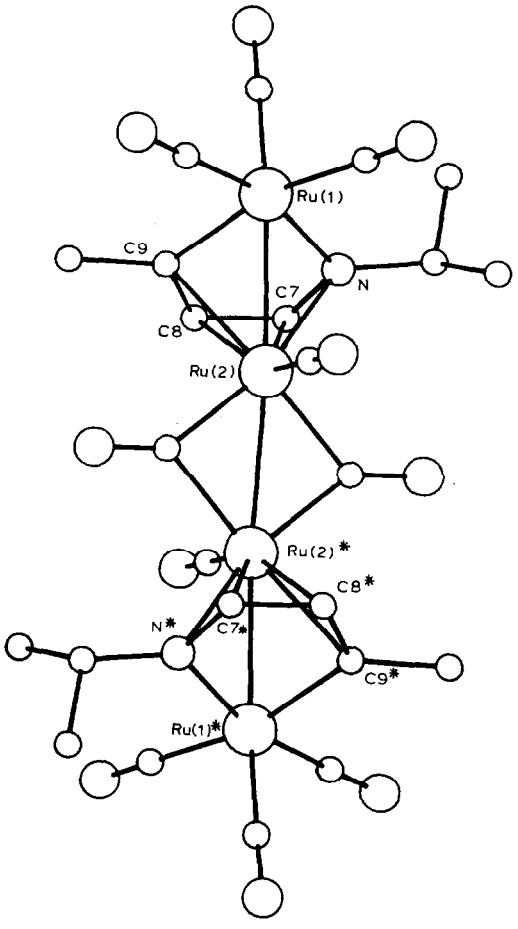

Fig. 12. Structure of $Ru_4(CO)_{10}$(i-Pr-N=C(H)(H)C=CCH_3).

group, while the Ru–Ru bond (2.650(1) Å is bridged by an η^3-azaallyl bonded NCC unit (Ru(1)–N 2.216(5), Ru(1)–C(7) 2.240(8), Ru(1)–C(8) 2.227(8), N–C(7) 1.404(10) and C(7)–C(8) 1.347(13) Å). Compound **B** (t-Bu) (Fig. 11) also contains a $Ru_2(CO)_6$ moiety (Ru–Ru 2.7980(4) Å) bridged by a rather interesting 6e donor ligand. This organic fragment bears on one side an N=C moiety σ-bonded to Ru(2) and on the other side an allene C(8)C(9)C(10) moiety, which is η^3-allyl bonded to Ru(1), while C(9) is also linked to Ru(2), this bonding type is thus very similar to that observed for $Ru_3(CO)_7$(neo-Pe-DAB)(C_3H_4) and for $Ru_2(CO)_5$(α-diimine)(C_3H_4) (α-diimine = c-Hex-DAB and c-Hex-Pyca) discussed before in this Review (Figs. 2 and 3).

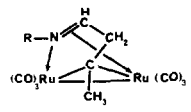

Fig. 13. Proposed structure of $Ru_2(CO)_6$(RN=C(H)(H)$_2$CCCH$_3$) (R = i-Pr or c-Hex).

The crystal structure of **C** (i-Pr) (Fig. 12) shows an approximately linear chain of four Ru atoms (Ru(1)–Ru(2) 2.7086(4), Ru(2)–Ru(2)* 2.7817(4) Å) with the latter bond bridged by two CO groups and the two terminal Ru–Ru bonds bridged by an 8e donor NCCC skeleton. The bonding of this skeleton (Ru(2)–C(7) 2.301(6), Ru(2)–C(8) 2.312(5), Ru(2)–C(9) 2.364(4) and Ru(2)–N 2.311(4) Å) is thus very similar indeed to the 8e-bonding of R-DAB in e.g. $H_2Ru_4(CO)_8$(R-DAB)$_2$ (Fig. 4). This is not surprising, since the $[RN{=}C(H)(H)C{=}CCH_3]^-$ anion is isoelectronic with R-DAB.

It is assumed that the proposed structure of **D** (i-Pr, c-Hex) (Fig. 13) contains a $Ru_2(CO)_6$ moiety with terminal CO groups and with a bridging RN=C-$(H)(H)_2CCCH_3$ moiety which acts as a 6e donor. The imine unit is σ-bonded to one Ru atom and η^2-bonded to the other Ru atom. The CH_2CCH_3 part of the organic fragment is bonded as μ_2-carbene fragment with the central C atom bridging over both Ru atoms.

We will not discuss these preliminary results further, but should point out that in the case of the enimine compounds H-abstraction and H-migration are facile processes.

Acknowledgements

I wish first to thank Prof.dr. G. van Koten, to whom I am much indebted for his cooperation in all aspects of the research. I also thank my coworkers Drs. L.H. Staal, J.J. Keijsper, L.H. Polm and R. Zoet for their enthusiastic research efforts.

References

1 G. van Koten and K. Vrieze, Recl. Trav. Chim. Pays-Bas, 100 (1981) 129.
2 G. van Koten and K. Vrieze, Adv. Organomet. Chem., 21 (1982) 151.
3 K. Vrieze and G. van Koten, Inorg. Chim. Acta, 100 (1985) 79.
4 C.J.M. Huige, A.L. Spek and J.L. de Boer, Acta Cryst., C41 (1985) 113.
5 J.J. Keijsper, H. van der Poel, L.H. Polm, G. van Koten and K. Vrieze, Polyhedron, 2 (1983) 1111.
6 O. Exner and J.M. Kliegman, J. Org. Chem., 36 (1971) 2014.
7 H. tom Dieck and I.W. Renk, Chem. Ber., 104 (1971) 92.
8 O. Borgen, B. Mestvedt and I. Skanvik, Acta Chem. Scand., Ser. A. 30 (1976) 43.
9 R. Benedix, R. Birner, F. Birnstock, H. Hennig and H.-J. Hofmann, J. Mol. Struct., 51 (1979) 99.
10 J. Reinhold, R. Benedix, P. Birner and H. Hennig, Inorg. Chim. Acta, 33 (1979) 209.
11 J.N. Louwen, D.J. Stufkens and A. Oskam, J. Chem. Soc., Dalton Trans., (1984) 2683.
12 J.J. Keijsper, L.H. Polm, G. van Koten, K. Vrieze, P.F.A.B. Seignette and C.H. Stam, Inorg. Chem., 24 (1985) 518.
13 J.J. Keijsper, L.H. Polm, G. van Koten, K. Vrieze, G. Abbel and C.H. Stam, Inorg. Chem., 23 (1984) 2142.
14 L.H. Staal, L.H. Polm, K. Vrieze, F. Ploeger and C.H. Stam, Inorg. Chem., 20 (1980) 3590.
15 H.W. Frühauf, A. Lander, R. Goddard and C. Krueger, Angew. Chem., 90 (1978) 56.
16 L.H. Polm, G. van Koten and K. Vrieze, to be published. See also ref. 12.
17 R. Zoet, G. van Koten, K. Vrieze and C.H. Stam, to be published.
18 L.H. Polm, G. van Koten, C.J. Elsevier, K. Vrieze, B.K.F. van Santen and C.H. Stam, to be published.
19 L.H. Polm, G. van Koten and K. Vrieze, to be published.
20 J.J. Keijsper, L.H. Polm, G. van Koten, K. Vrieze, K. Goubitz and C.H. Stam, Inorg. Chim. Acta, in press.
21 W.A. Herrmann, Adv. Organomet. Chem., 20 (1982) 159.
22 J.J. Keijsper, L.H. Polm, G. van Koten, K. Vrieze, E. Nielsen and C.H. Stam, Organometallics, in press.

23 L.H. Staal, A. Oskam, K. Vrieze, E. Roosendaal and H. Schenk, Inorg. Chem., 18 (1979) 1634.
24 L.H. Staal, L.H. Polm, R.W. Balk, G. van Koten, K. Vrieze, and A.M.F. Brouwers, Inorg. Chem., 19 (1980) 3343.
25 J.J. Keijsper, G. van Koten, K. Vrieze, M. Zoutberg and C.H. Stam, Organometallics, 4 (1985) 1306.
26 R.D. Adams, J. Am. Chem. Soc., 102 (1980) 7476.
27 G. van Koten, J.T.B.H. Jastrzebski and K. Vrieze, J. Organomet. Chem., 250 (1983) 49.
28 J.T.B.H. Jastrzebski, J.M. Klerks, G. van Koten and K. Vrieze, J. Organomet. Chem., 210 (1981) C49.
29 J.J. Keijsper, L.H. Polm, G. van Koten, K. Vrieze, C.H. Stam and J.D. Schagen, Inorg. Chim. Acta, 103 (1985) 137.
30 L.H. Staal, G. van Koten, K. Vrieze, B. van Santen and C.H. Stam, Inorg. Chem., 20 (1981) 3598.
31 J. Piron, J. Meunier-Piret and M. van Meerssche, Bull. Soc. Chim. Belg., 78 (1969) 121.
32 L.H. Polm, G. van Koten, K. Vrieze, C.H. Stam, and W.C.J. van Tunen, J. Chem. Soc., Chem. Commun., (1983) 1177.
33 L.H. Staal, G. van Koten and K. Vrieze, J. Organomet. Chem., 175 (1979) 73.
34 L.H. Staal, J.J. Keijsper, G. van Koten, K. Vrieze, J.A. Cras and W.P. Bosman, Inorg. Chem., 20 (1981) 555.
35 J.J. Keijsper, P. Grimberg, G. van Koten, K. Vrieze, B. Kojić-Prodić and A.L. Spek, Organometallics, 3 (1985) 438.
36 J.J. Keijsper, J. Mul, G. van Koten, K. Vrieze, H.C. Ubbels and C.H. Stam, Organometallics, 2 (1984) 1732.
37 J.J. Keijsper, P. Grimberg, G. van Koten, K. Vrieze, M. Christophersen and C.H. Stam, Inorg. Chim. Acta, 102 (1985) 29.
38 L.H. Polm, G. van Koten, C.J. Elsevier and K. Vrieze, to be published.